Voltage Stability Assessment in Semi-Autonomous DC-Grids with Multiple Power Modules

K. Rykov [1] , J.L. Duarte [1], U. Boeke [2], M. Wendt [2], and R. Weiss [3]
[1] Eindhoven University of Technology, [2] Philips Research Europe, [3] Siemens Aktiengesellschaft
Eindhoven University of Technology
P. O. Box 513
5600MB Eindhoven The Netherlands
Phone: +31 (0) 40 247-3504
Email: k.rykov@tue.nl
URL: http://www.tue.nl; http://www.dcc-g.eu

Acknowledgments

The authors would like to thank ENIAC, DCC+G project members for the financial support and cooperation.

Keywords

≪Semi-autonomous DC-grids≫, ≪Voltage instability analysis≫, ≪Impedance identification≫, ≪Droop control≫, ≪Nyquist stability criterion≫, ≪Matlab/Simulink≫.

Abstract

Basic concepts with respect to stable operation of semi-autonomous low-voltage DC-grids are discussed. Design considerations on the output impedances of power electronic converters are analysed in order to avoid resonance issues within a DC-grid. With calculated or measured converter output impedances, potential resonance problems due to background harmonics between aggregated power modules and the DC-grid can be forecasted. Simulation results are included for verification of the proposed ideas.

Introduction

Low-voltage DC-grids with up to 1500 V DC are conceived as an enabling technology to integrate (sustainable) electricity sources, energy storage devices and a variety of loads in an efficient way [1]. The system design and integration require a variability of operating conditions and, therefore, system stability issues may arise from dynamical interactions among multiple components, which are normally designed to meet their own stability requirements [2]. As the result, after the system integration, interactions among modules can lead to instabilities in the DC-grid [3].

Since the application of low-voltage DC-grids in commercial buildings is of quite recent date, there are not yet well developed techniques for system studies, especially when multiple energy sources and loads are present [4,5]. The quality of the voltage along the whole power network should be guaranteed constantly, and for this purpose it is also necessary to forecast by means of simulations the impact of different load scenarios on voltage transients.

There have been attempts of modelling DC-grids in the past, for instance, for data-base storage systems. However, the proposed techniques up to now only consider the output impedance of the required power electronic converters, and do not take into account the effect of the converter control algorithms. Nevertheless, the latter is an essential aspect that may not be disregarded in order to describe voltage instability when many converters are interacting with each other.

When including the impact of the control algorithms of the individual power processing converters, the processing time for obtaining meaningful results with standard simulation tools, like MatLab/Simulink

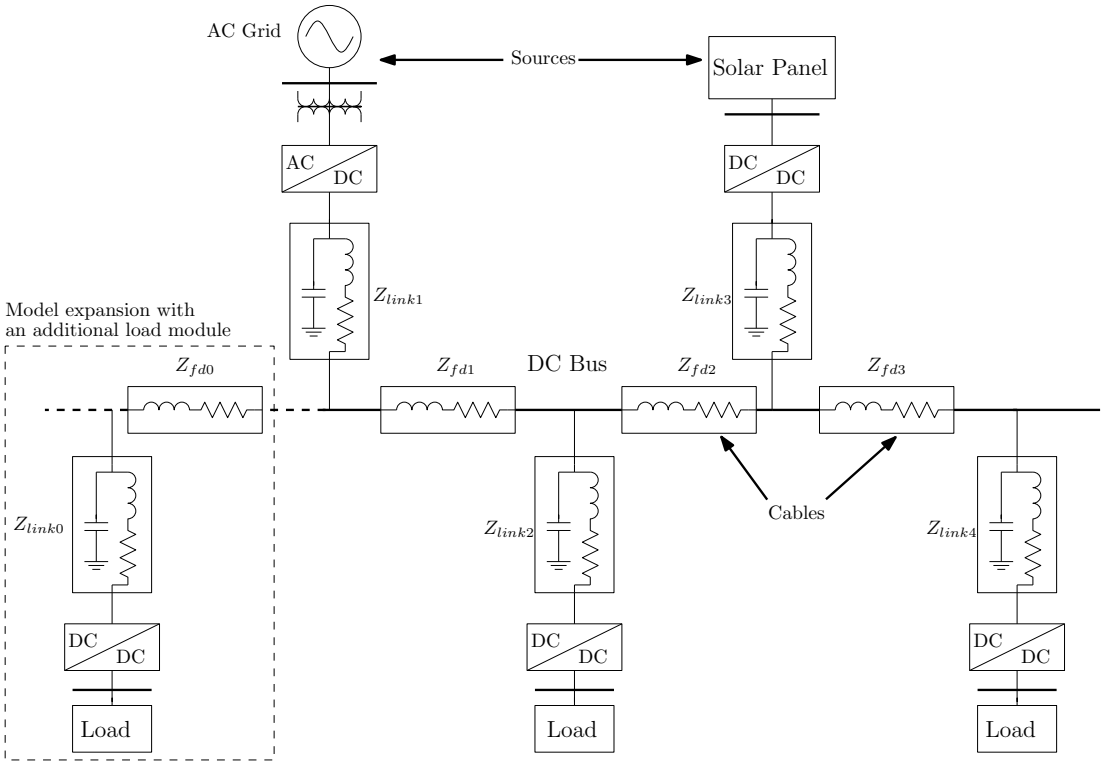

Fig. 1: Semi-autonomous DC-grid with heterogeneous source and load modules.

or LTSpice, is prohibitive. Starting from existing techniques available for AC micro-grids, in this paper the description of a simulation program for voltage stability assessment in DC-grids with an arbitrary number of sources and loads is presented. The approach focuses on the forecast of voltage instability at each point of common coupling in the DC network. For this purpose an impedance identification technique is applied that subsequently enables for a relatively simple and effective data analysis using such control engineering theory techniques as the Nyquist Stability Criterion and Bode Plots analysis. The resulting software tool is supposed to provide essential information for system designers to consider different load scenarios and the extension of existing small-scale grids with a considerable number of sources and loads.

System Modeling

In semi-autonomous DC-grids some of the power modules are actively controlled by converters with bidirectional power flow capability connected to a larger AC-network. An example of a simplified semi-autonomous micro-grid is illustrated in Fig. 1.

The AC-interfacing converters, usually named slack terminals, are applied – in combination with energy storage devices connected to bidirectional DC/DC converters – to actively balance the power flow. For this purpose, a cascaded control scheme is normally employed, where an outer voltage loop is cascaded with an inner current/power loop and corresponding PWM modulation process, as shown in Fig. 2.

The proper modelling of the converters and its corresponding control is one of the major issues for the analytical evaluation of a grid with multiple modules. Switching models incorporate the details of PWM modulation within each sampling cycle and are able to provide the closest simulation to real implementation. However, the inclusion of non-linear modulation details will make the modelling and simulation of a DC-network with an important number of converters extremely complicated and time-costly.

Average models [6], with the switching process neglected, enables the description of a DC-grid by means of linearised transfer functions. However, the derivations are quite complicated especially when there are multiple slack terminals incorporated. For instance, in [7] the slack terminal on the receiving end of a back-to-back DC system is modelled as an equivalent resistance which represents its droop regulator with additional filter incorporated. Droop control method enables for avoiding real-time inter-communication

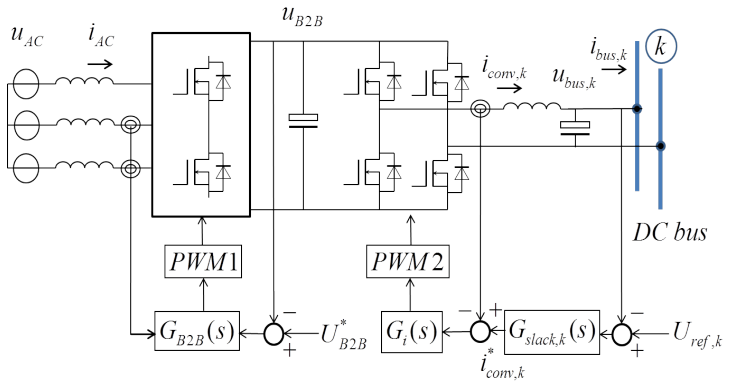

Fig. 2: Detailed schematics of the slack terminal with cascaded control.

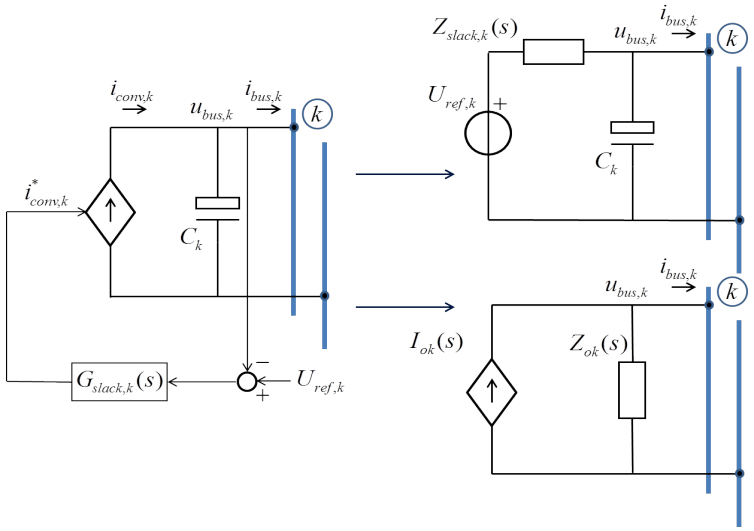

Fig. 3: Modelling a slack terminal that incorporates a bidirectional converter with cascaded control(left); Norton and Thevenin equivalents (right).

of several energy sources with a central controller and operating autonomously on the same bus [9]. Nevertheless, a single equivalent resistance cannot represent correctly the terminal dynamics of the converter.

In this paper, an alternative approach is described for the voltage stability assessment of converter interfaced DC networks. Using the proposed method, the dynamics of the actively controlled converters can be modelled as equivalent impedances in frequency domain, and the analysis of system behaviour can therefore be transformed into a simpler circuit analysis. As a consequence, known circuit techniques, e.g. Thevenin or Norton equivalent impedances (Fig.3 (right)), can be used to assess the stability and dynamics [8].

As an example of the proposed modelling procedure, the method for describing a slack module is illustrated in Fig. 3, consisting of a bidirectional DC/DC converter as in Fig. 2.

The switching frequency of the converter bridge in Fig. 3 is assigned much higher than the possible grid resonance frequencies. Therefore, the switching period can be averaged. Furthermore, the output inductor current of the converter in Fig. 2 is usually controlled by a fast single-loop inductor current feedback with PI compensator, which is widely used in existing designs because of its simplicity. Corresponding control scheme of the converter module is shown in Fig. 4. The transfer function of the PI controller is found to be

$$G_{slack,k}(s) = K_p + \frac{K_i}{s}, \text{ where } K_p \text{ and } K_i \text{ are proportional and integral gains correspondingly.}$$

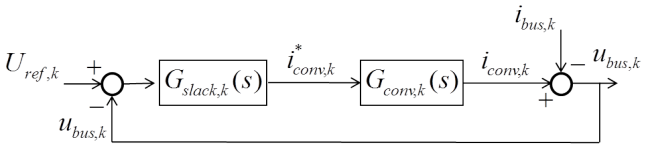

Fig. 4: Control scheme of a slack module.

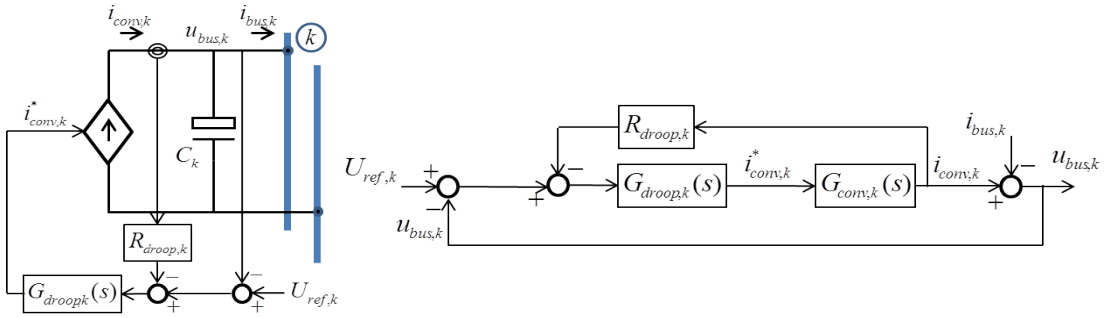

Fig. 5: (a) Droop control module schematics; (b) Control diagram of a droop module.

The converter module together with the current controller $G_i(s)$ in Fig.2 may be represented by just a unity current gain, including a propagation delay corresponding to several switching periods, as

$$G_{conv,k}(s) = \frac{i_{conv,k}(s)}{i^*_{conv,k}(s)} = \frac{1}{1+(nT_{sw})s}.$$

Altogether, the transfer function between the desired and measured voltages at the point of connection of the slack converter with the DC-bus can be described as a block diagram as shown in Fig. 5, where another PI compensator is applied for voltage correction. From the total transfer function of the converter $G_k(s) = G_{slack,k} \cdot G_{conv,k}(s)$ the resulting converter impedance expression can be derived as $Z_{slack,k}(s) = 1/G_k(s)$, and the output inductor current as

$$i_{conv,k}(s) = G_k(s)[U_{ref,k}(s) - u_{bus,k}(s)].$$

After a moment of reflection, it is possible to rewrite the block diagram in Fig. 3(left) as an equivalent impedance representation, shown in Fig. 3(right), where the gains in the control diagram become frequency-dependent impedances, and the voltage reference becomes a constant voltage source [8].

Finally, from Fig.3 and Fig.4 the frequency-dependent Norton-equivalent representation of the interface converter is straightforward to be obtained, yielding the network components - equivalent current $I_{ok}(s)$ and impedance $Z_{ok}(s)$ - where

$$I_{ok}(s) = \frac{U_{ref,k}(s)}{Z_{slack,k}(s)}, \qquad Z_{ok}(s) = Z_{slack,k}(s)//[1/sC_k]. \tag{1}$$

The same approach can be applied to derive Norton-equivalents of other source modules with local voltage droop control, or to local constant power load modules. Droop control module and the control diagram are depicted on Fig. 5(a) and Fig. 5(b) correspondingly. Similarly to the slack module, the converter output inductor current is controlled by PI controller with the transfer function $G_{droop}(s) = K_p + K_i/s$. From the control diagram (Fig. 5(b)) the total converter impedance follows as

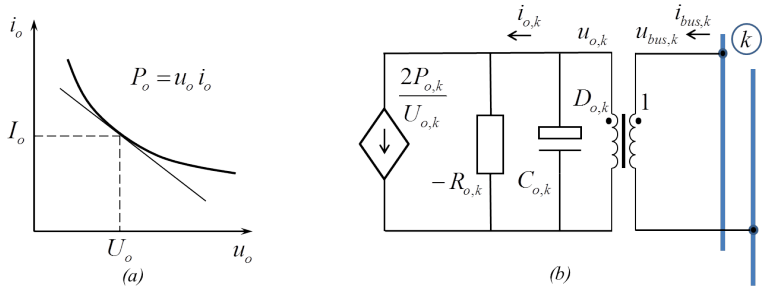

Fig. 6: (a) Load with constant output power; (b) Load module circuit.

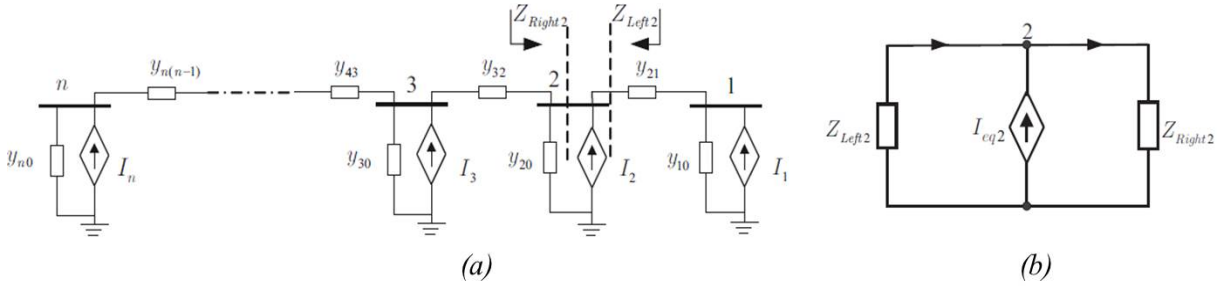

Fig. 7: (a) Grid admittance model; (b) Equivalent circuit model [8].

$$G_{droop,k}(s) = \frac{G_{droop,k}(s)G_{conv,k}(s)}{1 + R_{droop,k}(s)G_{droop,k}(s)G_{conv,k}(s)}, \qquad Z_{droop,k}(s) = \frac{1}{G_k(s)}.$$

Norton equivalent parameters for the droop control module are derived in the same way as for the slack module in (1), with

$$I_{ok}(s) = \frac{U_{ref,k}(s)}{Z_{droop,k}(s)}, \qquad Z_{ok}(s) = Z_{droop,k}(s)//[1/sC_k].$$

Small-signal analysis can be used for the load modules. Output characteristics of the load with constant output power can be linearised within the small deviation of the signal (Fig. 6(a)). Considering the circuit of the load module showed in Fig. 6(b), an expression for the output current, which can be used subsequently in the Norton equivalent, is steadily derived from

$$i_o = I_o - \frac{I_o}{U_o}(u_o - U_o), \qquad i_o \approx \frac{2P_o}{U_o} - \frac{1}{R_o}u_o.$$

Once the Norton-equivalent frequency-dependent impedances of all source and load modules connected to the common DC-bus are known, the method described in [8] can be applied to derive the resulting lateral impedances at any node. Taking Node 2 as an example, Fig. 7 shows the possibility to obtain an equivalent circuit from the grid admittance model. Consequently, impedances to the left, Z_{Left2}, and to the right, Z_{Right2}, from the point of connection can be obtained, which give a basis to forecast harmonic resonances using such control theory techniques as the Nyquist stability criterion or Bode Plots analysis.

Voltage Stability Analysis

In order to investigate and forecast possible voltage instabilities, a small-scale DC-grid model with four modules linked by cables is analysed with the PLECS toolbox for Matlab Simulink. For the first step, converters are represented as average models with the switching scheme neglected. It results in simplification of the model and faster performance. Nevertheless, including switching in converters makes

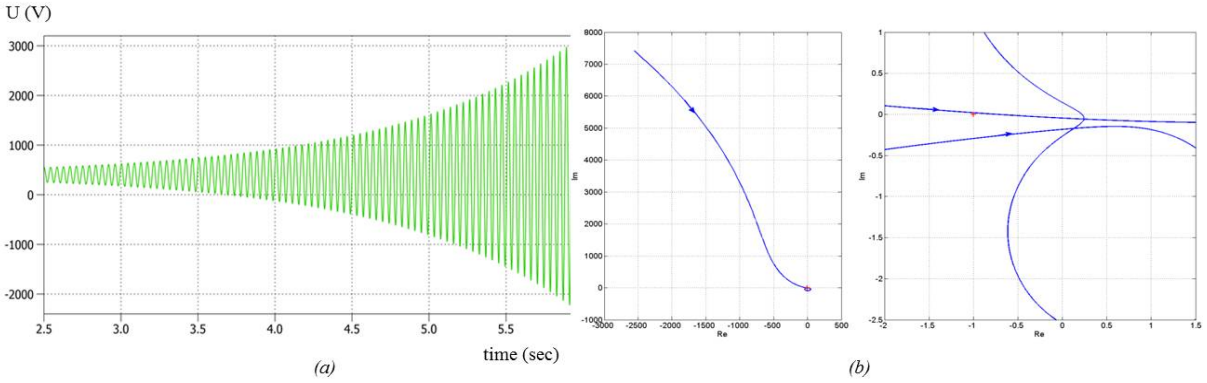

Fig. 8: (a) Simulated load step response at Node 2 with $Kp_{droop} = Kp_{slack} = 0.010; Ki_{droop} = Ki_{slack} = 30; C_2 = C_4 = 500\mu F$. (b) Corresponding Nyquist plots with different axis scaling.

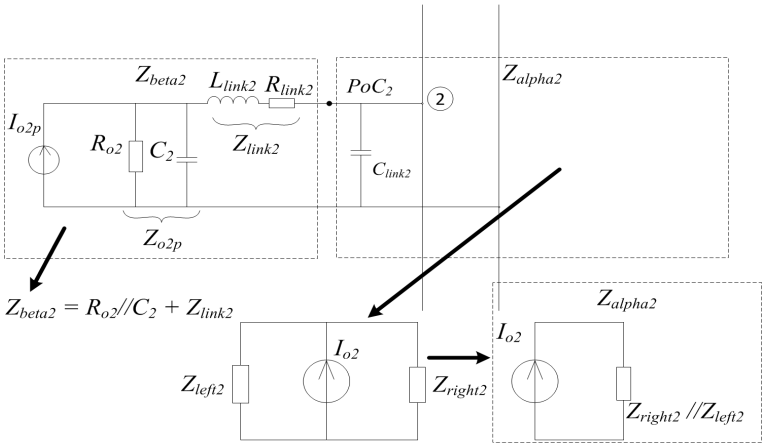

Fig. 9: System decomposition for Nyquist analysis.

the the behaviour of the system more realistic and representative. Therefore, the results obtained with average models have been confirmed afterwards by detailed switching simulations.

A Matlab script has been written in order to calculate the total lateral impedances for each of the four points of connection. With the resulting simplified system representation as in Fig. 7(a) – a current source and two impedances in parallel (Z_{left} and Z_{right}) in respect to the point of connection – analysis in frequency domain is readily performed to obtain Bode diagrams or Nyquist plots for the each node under specific load conditions.

The major parameters affecting the system stability in Fig. 4 are terminal capacitances $C_1 - C_4$ (load terminals are especially points of concern because of "negative" resistances and high values of power), proportional and integral gain components of the PI-controllers, and virtual droop resistances. As an illustration, system parameters are chosen in such way that it results in voltage instability. Corresponding load step response for $Kp_{droop} = Kp_{slack} = 0.010; Ki_{droop} = Ki_{slack} = 30; C_2 = C_4 = 500\mu F$ is shown in Fig. 8 and it is clearly visible that oscillations have increasing amplitude.

Nonetheless, in order to confirm the fact of instability, the Nyquist stability criterion can be applied. According to this criterion, the Nyquist Plot of the system in the frequency range from $\omega = 0$ to $\omega = \infty$

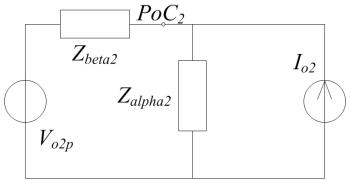

Fig. 10: Resulting circuit for Nyquist analysis.

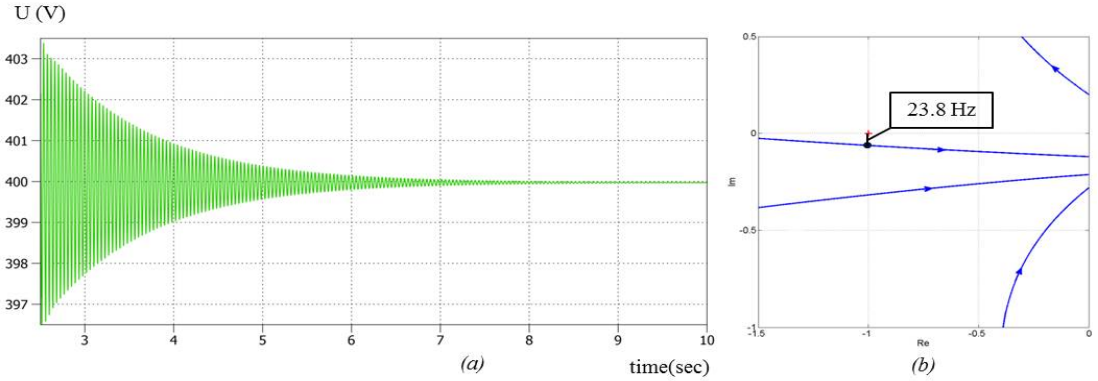

Fig. 11: Simulated load step response at Node 2 with $Kp_{droop} = Kp_{slack} = 0.015; Ki_{droop} = Ki_{slack} = 30; C_2 = C_4 = 500\mu F$. (b) Nyquist plot and the point of 23.8 Hz that corresponds to the closest vicinity of (-1;0).

must not cover the critical point (-1, 0) for achieving absolute stability. The proposed system description in sense of transfer functions should be adapted to let the approach be used. The idea is illustrated in Fig.9 as follows. The system is decomposed into two parts at the point of connection (PoC_2) of the load terminal 2, for instance (before the capacitor C_{link2} in Fig.9). As the result, two impedances Z_{alpha2} and Z_{beta_2} are obtained. Component Z_{alpha2} is composed by two parallel impedances Z_{left2} and Z_{right2}, which now comprise slightly different parts – Z_{left2} now involves only Z_{Clink2} in Z_{o2}. The component Z_{beta2} represents the series composition of Z_{o2p} and Z_{link2}. The resulting circuit is shown in Fig. 11, where the current source I_{o2p} in parallel with Z_{beta2} was substituted with the equivalent Thevenin voltage source V_{o2p} in series with Z_{beta2}. The transfer function of the circuit from the output V_{poc2} to the input V_{o2p} is derived as

$$\frac{V_{poc2}(s)}{V_{o2p}(s)} = \frac{Z_{alpha2}(s)}{Z_{alpha2}(s) + Z_{beta2}(s)} = \frac{1}{1 + \dfrac{Z_{beta2}(s)}{Z_{alpha2}(s)}}.$$

For the sake of stability analysis utilizing Nyquist stability criterion, the critical point (-1;0) should not be enclosed by the polar plot (the point should remain on the left side from the plot along the entire frequency range from $\omega = 0$ to $\omega = \infty$) of the transfer function $T_2(s) = \dfrac{Z_{beta2}(s)}{Z_{alpha2}(s)}$.

Therefore, both the step response (oscillation amplitude increases) and the Nyquist plot (the critical point (-1;0) is enclosed) confirm that the system is unstable. In order to make the system stable several parameters should be alternated. For this purpose, the analysis of the Nyquist plots corresponding to each network node is quite convenient. An example is given in Fig. 11, where the converters output capacitances C_2 and C_4 have been increased from $500\mu F$ to $1000\mu F$. It is important to mention that, as expected, the critical point (-1;0) in the Nyquist plot is now not enclosed any more in Fig. 11(b) and the voltage oscillations are damped (see Fig. 11(a)).

It is also illustrative to determine the frequency that corresponds to the point of the Nyquist plot that is situated in the closest vicinity of point (-1;0) as shown in Fig. 11(b). This is the dominant frequency of the voltage oscillations shown in Fig. 11(a). Further information about stability can be obtained from Bode plots of the resulting impedances (Fig. 12). Parallel resonance between Z_{Left} and Z_{right} may occur when the sum of the impedances is at a minimum resistive value (that is to say, when the phase characteristics in the Bode plot add to zero). This is presented in Fig. 12 and Fig. 13, where the oscillations of the output voltage of Node 2 can be recognized at following frequencies, including 23.8 Hz.

Consequently, the idea of this approach is that there is freedom of choice between several key parameters leading to system stability. Otherwise stated, when introducing new source/load modules into the DC grid, the system designer can decide the value of the minimum converter output capacitance that should be necessary, or whether changes on the converter control parameters are required.

Although the analysed DC-grid has only four modules, the proposed approach is suitable to study stability issues of DC micro-grids with a significant number of devices, like in commercial buildings or retail

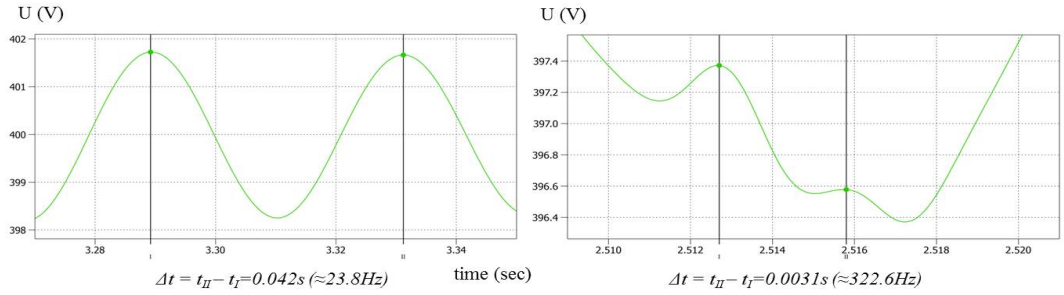

Fig. 12: Output voltage oscillations at the Node 2. The detail shown are zoomed views of the waveforms in Fig.11.

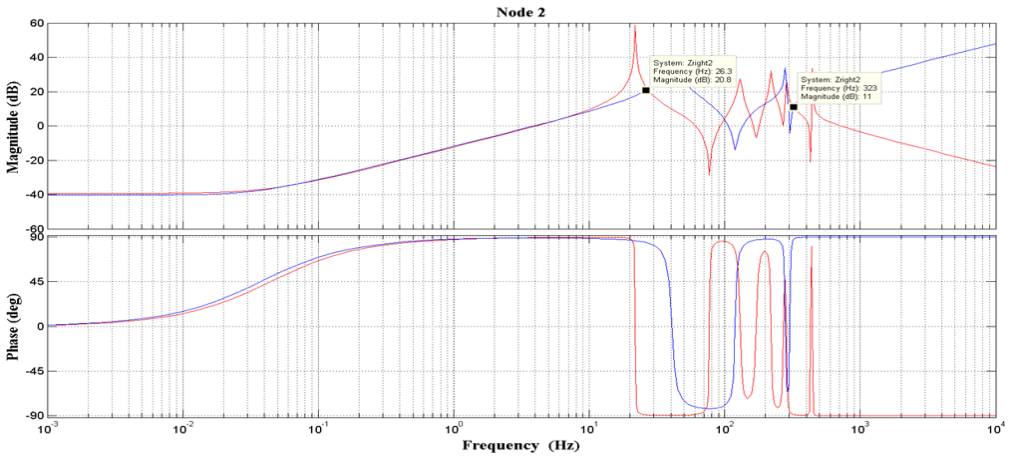

Fig. 13: Bode plots of Z_{left} and Z_{right} impedances at the Node 2.

shops. For the sake of analysis of the impact of increasing number of modules, let us consider the previous system with an additional load module of 1 kW (see Fig.1). Obviously, an extra impedance in the form of negative resistance is a potential source of instability in the grid. The corresponding Nyquist plot confirm the mentioned fact (see Fig. 14(a)). As it was mentioned above, implementation of the switching scheme to converters modules on one hand increase simulation time, but on another – makes the system more precise. The modified system with implemented hysteresis control both in slack modules (see Fig. 14(b)) and droop control modules was used for the simulations with an additional load module.

Experimental Impedance Identification

A modelling technique has been presented to analyse stability issues in small-scale DC-grid systems. In order to characterize the converter module impedances experimentally, a practical impedance identification method is introduced, which can be applied to already existing systems. The method is based on injecting of small-signal excitation AC-voltages of different frequencies [10], subsequent voltage measurements on both sides from the excitation, and processing the data using Fast Fourier Transform (FFT) techniques in order to obtain Bode plots of equivalent lateral impedances with respect to the excitation source (Fig. 15). Additionally, an experimental set-up was built to verify the proposed approach in practice (Fig. 15). The principle of the technique is the following. The circuit of the system under investigation containing a converter module, excitation voltage, voltage measurements and the load is shown in Fig. 16 (a). If the voltages $V_1(s)$ and $V_o(s)$ are measured, then using the ratio $v(s) = \dfrac{V_1(s)}{V_o(2)}$ together with the impedances $Z_1(s)$ and $Z_o(s)$, the internal converter impedance $Z_{conv}(s)$ can be obtained utilizing the expression as follows

$$Z_{conv}(s) = -\frac{v(s)Z_o(s)Z_1(s)}{Z_1(s)+v(s)Z_o(s)}.$$

Similarly, in order to identify the DC-grid equivalent impedance $Z_o(s)$ knowing the measured voltage ratio $v(s)$ and impedances $Z_1(s)$ and $Z_{conv}(s)$, the following expression can be used

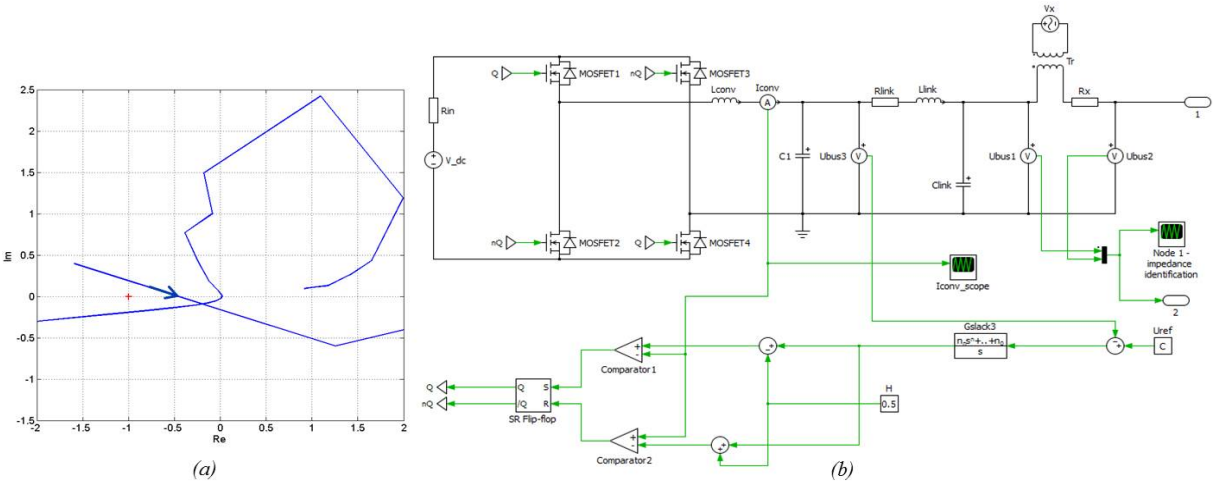

Fig. 14: (a) Nyquist plot for the system in Fig.1 with an additional load module; (b) PLECS schematics of the slack module with hysteresis control.

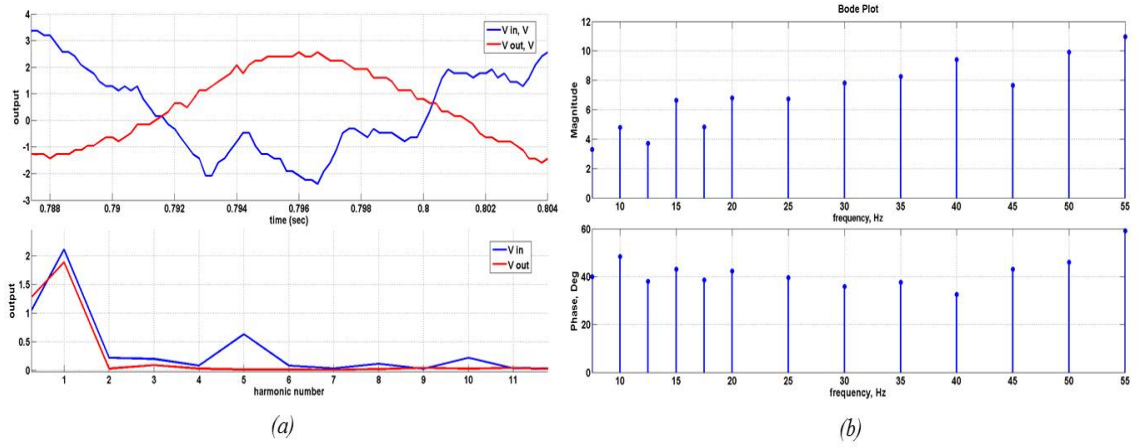

Fig. 15: (a) Measured voltage waveforms on the both sides of excitation together with FFT plot; (b) Obtained Bode plot of the system.

$$Z_o(s) = -\frac{1}{v(s)} \cdot \frac{Z_1(s) Z_{conv}(s)}{Z_1(s) + Z_{conv}(s)}.$$

It is important to mention that values of $V_x(s)$ and $Z_x(s)$ (voltage and internal impedance of the excitation source) are not essential for the identification. Thus, the method gives the opportunity to obtain internal impedance information of a converter without knowing the structure of the converter itself. Future work relates to extension of the existing theoretical and experimental systems and improvement of software flexibility.

Conclusions

A method is proposed to analyse voltage stability issues in small-scale DC-grids, which accommodate heterogeneous sources and loads. Preliminary simulation results confirm that it is possible to forecast the origin of unstable voltage oscillations on the basis of equivalent converter impedances. The presented analysis approach allows choosing converter control parameters or output capacitances which yield stable grid operation. Detailed numerical simulation results verify the proposed ideas.

A model of a small-scale DC-grid containing two loads and two sources represented as Norton equivalents was built. Impedance information of each module combined into an impedance matrix provides the possibility to analyse the system behaviour at each network point utilizing the Nyquist stability cri-

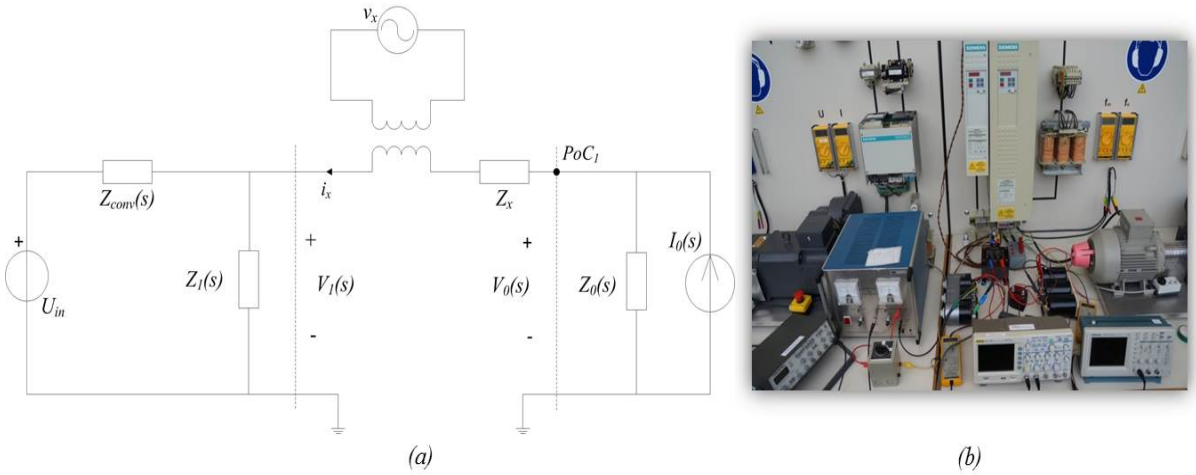

Fig. 16: (a) Impedance identification method applied to a single converter module; (b) Experimental set-up.

terion, frequency response and output characteristics. Moreover, the system model was verified with the switching scheme implementation and increased number of modules.

One of the important tasks was to develop a technique for transfer function analysis based on measurements of real signals. The experimental set-up is under development to exploit the method of practical impedance identification injecting small signal excitation AC voltages and carrying out voltage measurements on the both sides of excitation. The applied approach helps to obtain Bode plots of the converter modules, which subsequently were used for analysis. The next steps will be made in the direction of software generalization and conducting measurements in real commercial test-beds.

References

[1] B. Partterson, "DC, Come Home", IEEE Power & Energy Magazine, Nov\Dec 2012, pp. 60-69.

[2] D. Boroyevich, I. Cvetkovic, D. Dong, R. Burgos, Fei Wang, F. Lee, "Future Electronic Power Distribution Systems – A contemplative view", 12th International Conference on Optimization of Electrical and Electronic Equipment, OPTIM 2010, pp. 1369-1380.

[3] X. Feng, Z. Ye, K. Xing, F. Lee, and D. Borojevic, "Individual load impedance specification for a stable dc distributed power system", in Applied Power Electronics Conference and Exposition, APEC 1999, vol. 2, pp. 923-929.

[4] T. Tanaka, T. Serada, and T. Sakai, "Simulation analysis of dc power supply system stability", in Applied Power Electronics Conference and Exposition, 2001. APEC 2001, vol. 2, pp.759-764.

[5] S. Sudhoff, S. Glover, P. Lamm, D. Schmucker, and D. Delisle, "Admittance space stability analysis of power electronic systems", IEEE Transactions on Aerospace and Electronic Systems, vol. 36, no. 3, pp. 965-973, Jul 2000.

[6] A.A.A. Radwan and Y.A.-R.I Mohamed, "Linear Active Stabilization of Converter-Dominated DC Microgrids", IEEE Trans. on Smart Grids, vol.3, no.1, pp.203-216, March 2012.

[7] P. Karlsson, and J., Svensson, "DC bus voltage control for a distributed power system", IEEE Trans. on Power Electronics, vol. 18, no. 6, pp. 1405-1412, Nov. 2003.

[8] F. Wang, J.L. Duarte, M.A.M. Hendrix, P. F. Ribeiro, "Modeling and Analysis of Grid Harmonic Distortion Impact of Aggregated DG Inverters", IEEE Trans. on Power Electronics, vol. 26, no. 3, pp.786-797, March 2011.

[9] M. Rodrigues, G. Stahl, L. Corradini, D. Maksimovic , "Smart DC power management system based on software configurable power modules", IEEE Trans. on Power Electronics, vol. 28, no.4, pp. 1571-1586, April 2013.

[10] R.D. Middlebrook, "Measurement of loop gain in feedback systems", Int. J. Electronics, vol. 38, no. 4, pp. 485-512, 1975.